

Structures, luminescent and magnetic properties of a series of (3,6)-connected lanthanide–organic frameworks†

Cite this: *Dalton Trans.*, 2014, **43**, 1814

Yin-Ling Hou,^{a,b} Rui-Rui Cheng,^{a,b} Gang Xiong,^{a,b} Jian-Zhong Cui^b and Bin Zhao^{*a}

Through hydrothermal reactions with corresponding lanthanide nitrates and 4-(4-carboxyphenylsulfonyloxy)-3-methoxybenzoic acid (H₂vspc), seven novel three-dimensional (3D) lanthanide–organic frameworks ([Ln(vspc)(Hvspc)(H₂O)]_n [Ln = Pr (**1**), Eu (**2**), Gd (**3**), Tb (**4**), Dy (**5**), Ho (**6**) and Er (**7**)] have been synthesized and structurally characterized. All of them are isostructural and crystallize in the monoclinic crystal system, *P*2₁/*c* space group. Their structures feature a (3,6)-connected topological network, in which Ln³⁺ were connected by carboxylate groups to give a 1D lanthanide chain, and the adjacent chains are further spanned by vspc²⁻ and Hvspc⁻ anions to form a 3D framework. The luminescent properties and lifetimes of **2** (Eu^{III}), **4** (Tb^{III}), and **5** (Dy^{III}) have been studied, and the corresponding luminescent lifetimes are 0.53, 0.99 and 0.014 ms, respectively. The magnetic investigations reveal that compound **3** displays weak antiferromagnetic interaction, **4** and **5** exhibit ferromagnetic coupling, and compound **5** exhibits slow magnetic relaxation behavior.

Received 22nd August 2013,
Accepted 15th October 2013

DOI: 10.1039/c3dt52305e

www.rsc.org/dalton

Introduction

The constructions of metal–organic frameworks have attracted much attention not merely because of their tunable synthesis and fascinating structures,¹ but also for their potential applicability in gas adsorption and separation,² catalytic,³ molecule and ion sensors,⁴ optic,⁵ electronic,⁶ and magnetic systems.⁷ Compared with the metal–organic frameworks based on transition metal ions, lanthanide–organic frameworks possess distinct superiority for the following reasons: (1) because of the high coordination numbers and flexible coordination geometries of Ln³⁺, it is easy to construct high connected lanthanide compounds with interesting topological structures - for example, the high 9-connected compound of [(2-*i*-PrC₆H₄-ORb)₆·(diox)_{4,5}] reported by Morris and co-workers,^{8a} and the unique (3,12)-connected topology discovered by our group.^{8b} (2) Originating from f–f transitions of their particular 4f

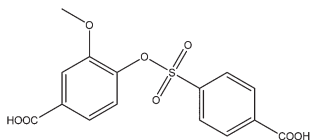
electrons shielded by outer electrons, lanthanide compounds usually possess extremely narrow peaks and long luminescent lifetimes,^{16,17} which is exploited for luminescent probes and laser materials.¹⁰ (3) Lanthanide compounds generally have unique magnetic properties due to strong unquenched orbital angular momentum of most of Ln³⁺,^{8c–g} which is supported by the fact that the single molecule magnetic (SMM) behavior is frequently observed in the lanthanide-based compounds.^{8b,c} (4) Ln³⁺ ions would be the one of the most competitive candidates for constructing multifunctional compounds due to their excellent luminescence, unique magnetic properties, porous properties including adsorption/exchanges and toxic substance separations *etc.* According to above four points, the lanthanide ions as metal centers were frequently selected to fabricate multifunctional metal–organic frameworks.^{3a,8e,9a}

It is well known that lanthanide ions are easily coordinated to oxygen atoms, and various organic carboxylate ligands have been usually employed to build lanthanide–organic frameworks, such as mono-, di- and poly-carboxylic acids.^{9,11} In this work, we used a dicarboxylic acid ligand with sulfonate group, 4-(4-carboxyphenylsulfonyloxy)-3-methoxybenzoic acid (H₂vspc) (Scheme 1), to construct 3D lanthanide–organic frameworks based on the following considerations: (1) there are two carboxylate groups that may be completely or partially deprotonated, yielding a variety of coordination modes and higher dimensional compounds with interesting structures; (2) the sulfonate group and methoxyl group may show additional steric hindrance due to their important geometric asymmetry;

^aDepartment of Chemistry, Key Laboratory of Advanced Energy Material Chemistry, MOE, TKL of Metal and Molecule Based Material Chemistry, and Synergetic Innovation Center of Chemical Science and Engineering (Tianjin), Nankai University, Tianjin 300071, China. E-mail: zhaobin@nankai.edu.cn

^bDepartment of Chemistry, Tianjin University, Tianjin, 300072, China

† Electronic supplementary information (ESI) available: Table of bond lengths and angles, TG curves, the emission spectrum of free H₂vspc ligand, luminescent decay curves of **2**, **4** and **5**, and other magnetic data. X-ray crystallographic files in cif format for compounds 1–7. CCDC 956810 (1), 956811 (2), 956812 (3), 956813 (4), 956814 (5), 956815 (6) and 956816 (7). For ESI and crystallographic data in CIF or other electronic format see DOI: 10.1039/c3dt52305e



Scheme 1 The structure of H₂vspc.

(3) compounds based on H₂vspc ligands have never been reported, as far as our information goes. Here, seven novel 3D lanthanide compounds, [Ln(vspc)(Hvspc)(H₂O)]_n [Ln = Pr (1), Eu (2), Gd (3), Tb (4), Dy (5), Ho (6) and Er (7)], were synthesized and characterized. All of them are isostructural and belong to the monoclinic crystal system, *P*2₁/*c* space group. The luminescent properties and lifetimes of 2 (Eu^{III}), 4 (Tb^{III}) and 5 (Dy^{III}) have been thoroughly studied. The magnetic investigations reveal that compound 5 displays slow magnetic relaxation behavior.

Experimental section

Materials and methods

All chemicals were commercially available, and used without further purification. The used water is distilled. Powder X-ray diffraction patterns were obtained on a D/Max-2500 X-ray diffractometer using Cu K α radiation. The Fourier transform infrared (FT-IR) spectra were recorded with a Bruker Tensor 27 spectrophotometer on KBr disks. The elemental analyses (C, H and N) were measured by a Perkin-Elmer elemental analyzer. Thermogravimetric analyses were determined on a Netzsch TG 209 TG-DTA analyzer from room temperature to 800 °C under nitrogen atmosphere with heating rate of 10 °C min⁻¹. The emission spectra in the visible region were conducted on a Cary Eclipse fluorescence spectrophotometer, and the luminescent lifetimes were taken on an Edinburgh Analytical Instrument F900. Variable-temperature magnetic susceptibilities were performed on a Quantum Design MPMS-XL7 magnetometer, and the alternating current (ac) magnetic measurements were performed on a PPMS-9 ACMS magnetometer. Diamagnetic corrections were made with Pascal's constants for all the constituent atoms.

X-ray diffraction studies

Suitable single crystals of 1–7 were mounted on an Oxford diffractometer SuperNova TM with a graphite-monochromatic MoK α radiation ($\lambda = 0.71073$ Å) using the ω -scan technique. All the structures were solved by direct methods and refined by full-matrix least-squares techniques based on F^2 using the SHELXS-97 and SHELXL-97 programs.¹² All the non-hydrogen atoms were refined with anisotropic parameters while H atoms were placed in calculated positions and refined using a riding model. ISOR and SIMU instructions in SHELXL were imposed on some carbon atoms and oxygen atoms to get reasonable displacement parameters in compounds 2–7. Detailed crystallographic data for 1–7 were summarized in Table 1. Selected

bond lengths and angles for 1–7 were listed in Table S1 and S2 (ESI[†]), respectively.

Synthesis

[Ln(vspc)(Hvspc)(H₂O)]_n [Ln = Pr (1), Eu (2), Gd (3), Tb (4), Dy (5), Ho (6) and Er (7)]. 0.05 mmol H₂vspc (0.0176 g), 0.1 mmol Ln(NO₃)₃·6H₂O [Ln = Pr (0.0435 g), Eu (0.0446 g), Gd (0.0451 g), Tb (0.0453 g), Dy (0.0457 g), Ho (0.0459 g) and Er (0.0461 g)], 0.25 mmol NH₄SCN (0.0190 g), and 8 mL H₂O were added to a 25 mL Teflon-lined stainless steel container and heated to 130 °C for 72 h under autogenous pressure, then cooled to room temperature in 72 h. Needle crystals were obtained and the yields are *ca.* 23% (1), 38% (2), 55% (3), 53% (4), 50% (5), 42% (6), and 35% (7) based on H₂vspc. Elemental analysis of C₃₀H₂₃O₁₇S₂Pr (1): calcd: C 41.87, H 2.69; found: C 41.68, H 2.82%; C₃₀H₂₃O₁₇S₂Eu (2): calcd: C 41.34, H 2.66; found: C 41.49, H 2.48%; C₃₀H₂₃O₁₇S₂Gd (3): calcd: C 41.09, H 2.64; found: C 41.25, H 2.67%; C₃₀H₂₃O₁₇S₂Tb (4): calcd: C 41.01, H 2.64; found: C 41.32, H 2.50%; C₃₀H₂₃O₁₇S₂Dy (5): calcd: C 40.85, H 2.63; found: C 40.64, H 2.81%; C₃₀H₂₃O₁₇S₂Ho (6): calcd: C 40.73, H 2.62; found: C 40.55, H 2.79%; C₃₀H₂₃O₁₇S₂Er (7): calcd: C 40.63, H 2.61; found: C 40.36, H 2.84%; IR spectra (KBr, cm⁻¹): compound 1: 3479 (br), 1697 (s), 1618 (s), 1552 (m), 1399 (vs), 1270 (w), 1192 (m), 1165 (m), 1110 (m), 1090 (m), 1034 (w), 870 (m), 776 (m), 713 (w), 613 (w), 543 (w); compound 2: 3515 (br), 1698 (s), 1600 (s), 1552 (m), 1419 (vs), 1278 (w), 1200 (m), 1157 (m), 1112 (m), 1087 (m), 1029 (w), 871 (m), 783 (m), 713 (w), 615 (w), 548 (w); compound 3: 3484 (br), 1691 (s), 1615 (s), 1542 (m), 1410 (vs), 1268 (w), 1195 (m), 1155 (m), 1114 (m), 1092 (m), 1031 (w), 873 (m), 780 (m), 716 (w), 609 (w), 538 (w); compound 4: 3500 (br), 1695 (s), 1614 (s), 1549 (m), 1408 (vs), 1275 (w), 1189 (m), 1158 (m), 1109 (m), 1085 (m), 1031 (w), 869 (m), 774 (m), 710 (w), 616 (w), 540 (w); compound 5: 3469 (br), 1688 (s), 1609 (s), 1546 (m), 1389 (vs), 1265 (w), 1200 (m), 1163 (m), 1115 (m), 1093 (m), 1030 (w), 865 (m), 768 (m), 709 (w), 608 (w), 535 (w); compound 6: 3499 (br), 1687 (s), 1621 (s), 1545 (m), 1394 (vs), 1268 (w), 1193 (m), 1160 (m), 1109 (m), 1085 (m), 1027 (w), 863 (m), 770 (m), 717 (w), 619 (w), 537 (w); compound 7: 3484 (br), 1693 (s), 1619 (s), 1557 (m), 1406 (vs), 1275 (w), 1194 (m), 1159 (m), 1114 (m), 1091 (m), 1030 (w), 877 (m), 766 (m), 709 (w), 617 (w), 533 (w).

Results and discussion

Description of structures

Single crystal X-ray diffraction analyses reveal that compounds 1–7 are isostructural and crystallize in the monoclinic crystal system, *P*2₁/*c* space group. Thus, compound 5 as a representative example is selected to describe the crystal structures in details. In compound 5, the asymmetric unit consists of one independent Dy³⁺, one full deprotonated vspc²⁻ anion, one half deprotonated Hvspc⁻ anion, and one coordinated H₂O molecule (Fig. 1). The eight-coordinated Dy³⁺ is surrounded by two monodentate O atoms (O3 and O4A) from two different

Table 1 Crystallographic data for compounds 1–7

| Compound | 1 (Pr) | 2 (Eu) | 3 (Gd) | 4 (Tb) | 5 (Dy) | 6 (Ho) | 7 (Er) |
|---|---|---|---|---|---|---|---|
| Formula | C ₃₀ H ₂₃ O ₁₇ S ₂ Pr | C ₃₀ H ₂₃ O ₁₇ S ₂ Eu | C ₃₀ H ₂₃ O ₁₇ S ₂ Gd | C ₃₀ H ₂₃ O ₁₇ S ₂ Tb | C ₃₀ H ₂₃ O ₁₇ S ₂ Dy | C ₃₀ H ₂₃ O ₁₇ S ₂ Ho | C ₃₀ H ₂₃ O ₁₇ S ₂ Er |
| Fw | 860.51 | 871.56 | 876.85 | 878.52 | 882.10 | 884.53 | 886.86 |
| T (K) | 124(2) | 124(2) | 124(2) | 124(2) | 124(2) | 124(2) | 124(2) |
| Crystal system | Monoclinic |
| Space group | <i>P</i> 2 ₁ / <i>c</i> |
| <i>a</i> (Å) | 23.4546(7) | 23.428(2) | 23.4006(7) | 23.3952(15) | 23.3391(5) | 23.327(2) | 23.318(2) |
| <i>b</i> (Å) | 14.1658(6) | 14.0753(13) | 14.1988(5) | 14.0348(11) | 14.0385(4) | 14.0248(11) | 14.0046(15) |
| <i>c</i> (Å) | 9.8960(4) | 9.8845(8) | 9.9356(4) | 9.8470(6) | 9.8581(3) | 9.8469(6) | 9.8371(10) |
| α (°) | 90 | 90 | 90 | 90 | 90 | 90 | 90 |
| β (°) | 95.692(3) | 94.907(8) | 94.468(3) | 94.930(6) | 94.703(2) | 94.653(7) | 94.552(9) |
| γ (°) | 90 | 90 | 90 | 90 | 90 | 90 | 90 |
| <i>V</i> (Å ³) | 3271.8(2) | 3247.5(5) | 3291.2(2) | 3221.3(4) | 3219.09(14) | 3210.9(4) | 3202.3(5) |
| <i>Z</i> | 4 | 4 | 4 | 4 | 4 | 4 | 4 |
| <i>D</i> _{calcd} (Mg m ⁻³) | 1.747 | 1.783 | 1.770 | 1.811 | 1.820 | 1.830 | 1.840 |
| μ (mm ⁻¹) | 1.696 | 2.140 | 2.221 | 2.406 | 2.532 | 2.675 | 2.832 |
| <i>F</i> (000) | 1720 | 1736 | 1740 | 1744 | 1748 | 1752 | 1756 |
| θ range (°) | 2.95/25.01 | 2.89/25.01 | 2.51/25.01 | 2.53/25.01 | 2.90/25.01 | 3.03/25.01 | 2.91/25.01 |
| Limiting indices | −20 ≤ <i>h</i> ≤ 27, −16 ≤ <i>k</i> ≤ 15, −10 ≤ <i>l</i> ≤ 11 | −27 ≤ <i>h</i> ≤ 27, −16 ≤ <i>k</i> ≤ 14, −11 ≤ <i>l</i> ≤ 11 | −27 ≤ <i>h</i> ≤ 23, −16 ≤ <i>k</i> ≤ 16, −11 ≤ <i>l</i> ≤ 11 | −27 ≤ <i>h</i> ≤ 27, −15 ≤ <i>k</i> ≤ 16, −11 ≤ <i>l</i> ≤ 11 | −20 ≤ <i>h</i> ≤ 27, −16 ≤ <i>k</i> ≤ 15, −10 ≤ <i>l</i> ≤ 11 | −27 ≤ <i>h</i> ≤ 23, −16 ≤ <i>k</i> ≤ 15, −11 ≤ <i>l</i> ≤ 11 | −27 ≤ <i>h</i> ≤ 25, −16 ≤ <i>k</i> ≤ 16, −11 ≤ <i>l</i> ≤ 11 |
| Reflections collected/unique | 13 564/5756 [<i>R</i> (int) = 0.0481] | 13 629/5719 [<i>R</i> (int) = 0.0816] | 13 237/5785 [<i>R</i> (int) = 0.0362] | 12 160/5681 [<i>R</i> (int) = 0.0413] | 12 334/5676 [<i>R</i> (int) = 0.0476] | 12 179/5655 [<i>R</i> (int) = 0.1060] | 13 502/5646 [<i>R</i> (int) = 0.1087] |
| Completeness to $\theta = 25.01$ | 99.8% | 99.8% | 99.9% | 99.9% | 99.9% | 99.8% | 99.9% |
| GOF on <i>F</i> ² | 1.055 | 1.061 | 1.056 | 1.036 | 1.033 | 1.017 | 1.045 |
| <i>R</i> ₁ ^a / <i>wR</i> ₂ ^b (<i>I</i> > 2 σ (<i>I</i>)) | 0.0496, 0.1046 | 0.0595, 0.1142 | 0.0431, 0.0963 | 0.0466, 0.1038 | 0.0485, 0.1043 | 0.0745, 0.1098 | 0.0691, 0.1021 |
| <i>R</i> ₁ / <i>wR</i> ₂ (all data) | 0.0710, 0.1169 | 0.1042, 0.1342 | 0.0586, 0.1061 | 0.0660, 0.1157 | 0.0698, 0.1174 | 0.1452, 0.1420 | 0.1459, 0.1391 |
| Largest diff. peak/hole (e Å ⁻³) | 1.501/−0.659 | 1.147/−0.846 | 1.229/−0.642 | 1.914/−0.780 | 1.986/−0.873 | 1.302/−1.032 | 1.757/−1.184 |

$$^a R_1 = \sum ||F_o| - |F_c|| / \sum |F_o|. \quad ^b wR_2 = \{ \sum [w(F_o^2 - F_c^2)^2] / \sum [w(F_o^2)^2] \}^{1/2}.$$

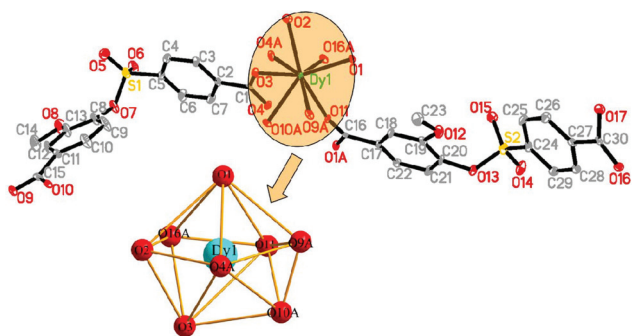
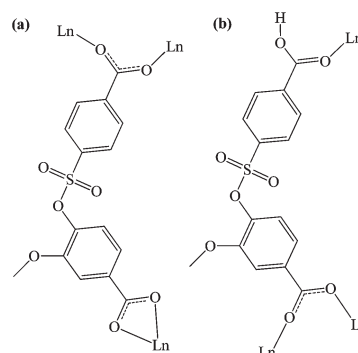


Fig. 1 The coordinated environments of Dy³⁺ in compound 5, all hydrogen atoms were deleted for clarity. A = −*x*, −0.5 + *y*, 2.5 − *z*.

vspc^{2−} anions, three monodentate O atoms (O1, O11, and O16A) coming from three different Hvspc[−] anions, two chelated O atoms (O9A and O10A) from one vspc^{2−} anion, and one O atom (O2) from one coordinated H₂O molecule, forming a distorted dodecahedron (Fig. 1). The Dy–O bond distances range from 2.255(5) to 2.538(4) Å, and the O–Dy–O angles are in the region of 52.61(14)–154.33(17)°, which fall into the Dy-based compounds range values reported previously.^{9a,11} In compound 5, vspc^{2−} and Hvspc[−] anions adopt different coordination modes, as shown in Scheme 2. The two



Scheme 2 Coordination modes of vspc^{2−} anion (a), and Hvspc[−] anion (b).

carboxylate groups of vspc^{2−} anion bridge two Dy³⁺ and chelate one Dy³⁺, respectively. For Hvspc[−] anion, one carboxylate group bridges two Dy³⁺, and the other without deprotonation links one Dy³⁺, in which the C–O_H and C–O_{Dy} bond length is 1.311 and 1.225 Å, respectively. The C–O bonds with significant difference suggest the H atoms located in the carboxylic groups were not removed, which was frequently observed in previous reports.^{9b,c}

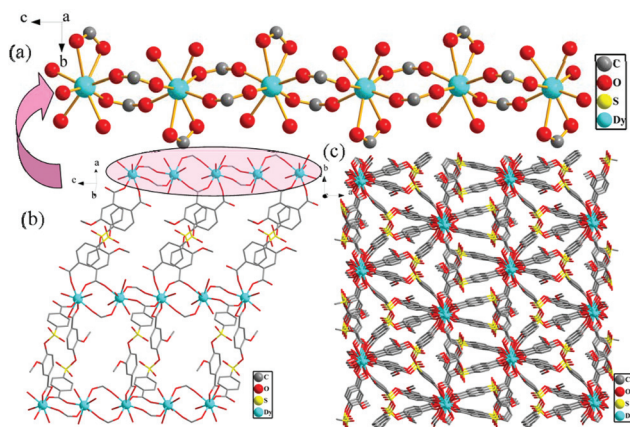


Fig. 2 (a) The 1D chain viewed along the *c* axis, (b) 2D plane, and (c) 3D framework in **5**. All hydrogen atoms were omitted for clarity.

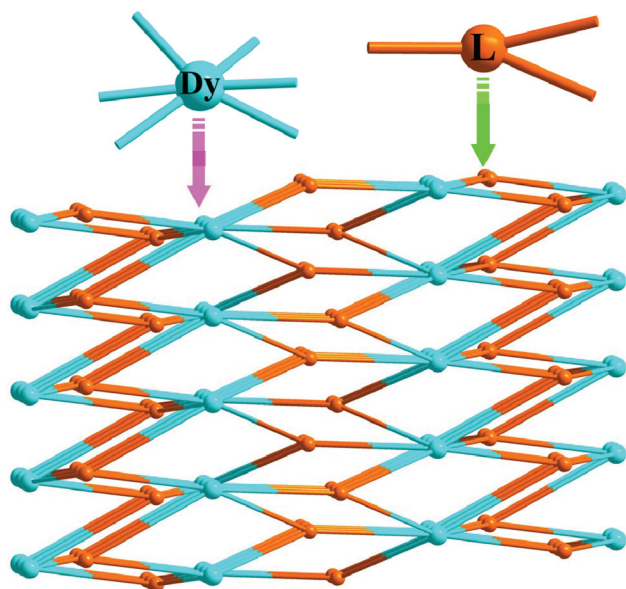


Fig. 3 The bi-nodal (3,6)-connected topological structure of **5**.

Two Dy^{3+} are spanned by two carboxyl groups to form a 1D chain along the *c* axis (Fig. 2(a)), and the Dy^{3+} – Dy^{3+} distance is 4.931 Å. The adjacent 1D chains are connected by ligands to generate a 2D plane (Fig. 2(b)), which further linked by ligands to give a 3D framework (Fig. 2(c)).

Topologically, both vspc^{2-} and Hvspc^{-} anions are regarded as 3-connected nodes, and the Dy^{3+} is considered as a 6-connected node. Thus the structure of **5** can be simplified as (3,6)-connected 3D framework, as shown in Fig. 3, giving the Schläfli symbol is $(4^2.6)_2(4^4.6^2.8^7.10^2)$, and the topological type is flu-3.

Powder X-ray diffraction (PXRD) and thermogravimetric analyses (TGA)

The purity of crystalline powders of **1–7** was confirmed by PXRD, and the results are shown in Fig. 4. The experimental

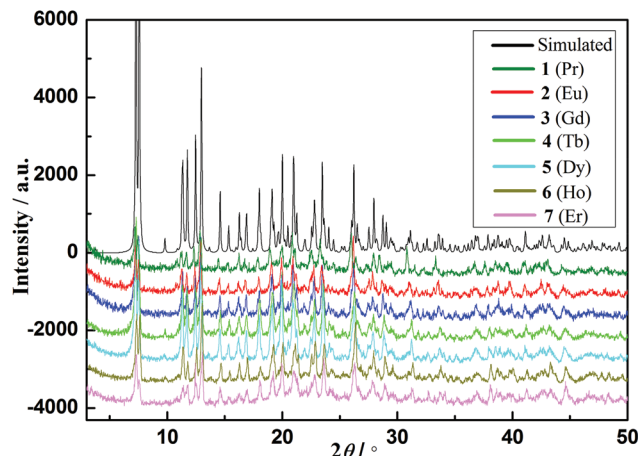


Fig. 4 The PXRD patterns of experimentation for **1–7** and simulation of **5**.

PXRD patterns of **1–7** are in accord with the corresponding simulated one obtained from the single-crystal data of compound **5**, indicating the purity of the solid samples.

The thermogravimetric analyses of **1–7** were measured under N_2 atmosphere by the heating rate of $10\text{ }^\circ\text{C min}^{-1}$, as shown in Fig. S1 (ESI[†]). The TG curves of **1–7** were similar since they are isomorphous. From room temperature to about $160\text{ }^\circ\text{C}$, no weight loss occurs, suggesting that there are no guest molecules in the 3D frameworks, which is also proved by single-crystal data. Between $160\text{ }^\circ\text{C}$ and $240\text{ }^\circ\text{C}$, the weight loss are 1.88%, 1.84%, 1.46%, 1.55%, 1.84%, 2.23% and 2.90%, corresponding to the theoretical value of removal one coordinated water molecule for **1–7** (**1**, 2.09%; **2**, 2.07%; **3**, 2.06%; **4**, 2.05%; **5**, 2.04%; **6**, 2.04%; **7**, 2.03%), respectively. After about $320\text{ }^\circ\text{C}$, the weight loss is sharp, indicating the decomposition of organic ligands and the collapse of the frameworks.

Luminescent properties

The luminescence properties of the solid H_2vspc ligand and compounds **2**, **4** and **5** were investigated at room temperature. Under the exciting wavelength of 320 nm, the H_2vspc ligand gives a maximum emitting peak at 362 nm (Fig. S2[†]), which is ascribed to the transition of $\pi^* \rightarrow \pi$.^{16a} The emission spectra of **2**, **4** and **5** are shown in Fig. 5, and they display the characteristic emissions of Eu^{3+} , Tb^{3+} and Dy^{3+} with the excitation of 285, 280 and 280 nm, respectively. For **2**, there are five emission peaks, 544, 592, 617, 654 and 699 nm, which are attributed to the transitions of $^5\text{D}_1 \rightarrow ^7\text{F}_1$, $^5\text{D}_0 \rightarrow ^7\text{F}_1$, $^5\text{D}_0 \rightarrow ^7\text{F}_2$, $^5\text{D}_0 \rightarrow ^7\text{F}_3$ and $^5\text{D}_0 \rightarrow ^7\text{F}_4$, respectively.^{8e,9a} According to the transition rules of Eu^{3+} , when it is in the centre of inversion, the transitions mainly are magnetic dipole transitions ($^5\text{D}_0 \rightarrow ^7\text{F}_1$), emitting the orange light; on the contrary, the electric dipole transitions ($^5\text{D}_0 \rightarrow ^7\text{F}_2$) are the major, emitting the red light. Comparing the transitions of $^5\text{D}_0 \rightarrow ^7\text{F}_1$ (592 nm) and $^5\text{D}_0 \rightarrow ^7\text{F}_2$ (617 nm) of **2**, the intensity ratio is about 1 : 5, suggesting that Eu^{3+} is in the low-symmetry and the centre of inversion

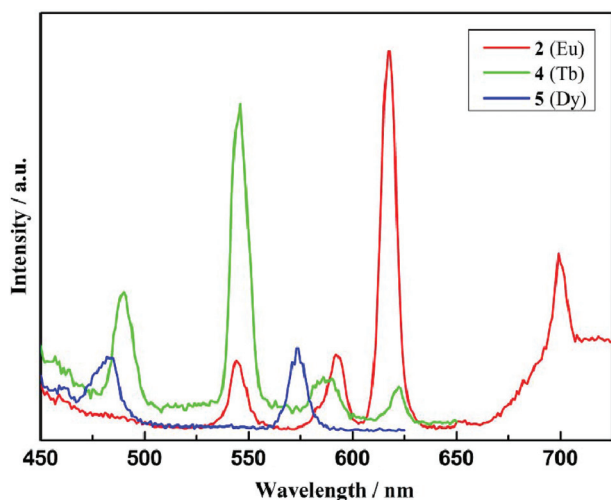


Fig. 5 The luminescent spectra of compounds 2, 4 and 5.

does not exist, which is in agreement with the results of the structural analyses.^{8e,9a,13} For 4, the four characteristic emission peaks of Tb³⁺ are 490, 546, 585 and 622 nm, belonging to transitions of ⁵D₄ → ⁷F_J (*J* = 6, 5, 4, 3), respectively, which are often observed in Tb-based compounds.^{8e,9a,13a} In the case of 5, only two characteristic emissions of Dy³⁺ are obtained in the visible region, which are ascribed to the transitions of ⁴F_{9/2} → ⁶H_{15/2} for 482 nm and ⁴F_{9/2} → ⁶H_{13/2} for 573 nm.^{8e,9a,13c}

The luminescence lifetimes of compounds 2, 4 and 5 were gauged under the excitation of 285 nm for 3, 280 nm for 4 and 5 at room temperature, and the plots of the luminescence decay of them are shown in Fig. S3†. For 2, 4 and 5, the decay curves of excited states of ⁵D₀ for Eu³⁺, ⁵D₄ for Tb³⁺ and ⁴F_{9/2} for Dy³⁺, monitored at 617, 546 and 573 nm, respectively, fit well with the monoexponential function: $I = A + B\exp(-t/\tau)$,¹⁴ where *A* and *B* are the fitting parameters, and τ is the luminescent lifetime, yielding the lifetimes are 0.53, 0.99 and 0.014 ms for 2, 4 and 5, respectively. The mono-exponential behavior of the luminescence decay curves for 2, 4 and 5 indicates one emission center exists in these compounds,¹⁵ which can be clearly explained by the crystal structures, in which there is only one crystallographic independent Ln³⁺ ion.

The luminescence lifetimes of 2 and 4 are moderate compared to some previous studies,^{9a,16} and both of them are in the millisecond order. For 5, the luminescence lifetime is much shorter than those of the previous reports,^{9a,17} and is only slightly longer than a few reported.¹⁸ That is because the coordinated water molecule can shorten the luminescence lifetime.^{18b,19}

Magnetic properties

Variable temperature magnetic susceptibilities of compounds 3–6 were investigated at the magnetic field of 1000 Oe in the temperature range of 2–300 K. The curves of $\chi_M T$ versus *T* are depicted in Fig. 6. For 3, the room temperature $\chi_M T$ value of 7.82 cm³ K mol⁻¹ is close to the theoretical value of 7.88 cm³ K mol⁻¹ for noninteracting Gd³⁺ (*S* = 7/2, *L* = 0, ⁸S_{7/2}, *g* = 2). As

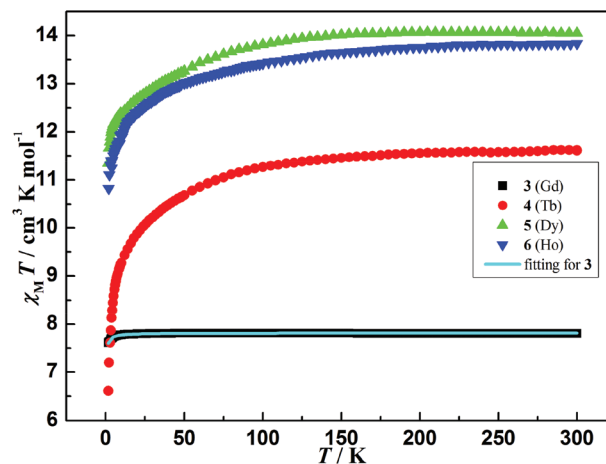


Fig. 6 The variable temperature magnetic susceptibilities of 3–6.

the temperature is decreased, the $\chi_M T$ value of 3 almost keeps constant until to 50 K, and then slightly decreases below 50 K to reach 7.61 cm³ K mol⁻¹ at 2 K, indicating antiferromagnetic interactions operate between adjacent Gd³⁺.

As described in the part of the crystal structures, Gd³⁺ ions were connected by carboxyl groups into a 1D chain structure in compound 3, and the Gd³⁺–Gd³⁺ distance is 4.969 Å, much shorter than the distance between adjacent 1D chains (longer than 13 Å). So, the magnetic interaction between 1D chains can be neglected, simplifying a 1D chain model. And the 1D chain model eqn (1) deduced by Fisher²⁰ could be used to quantitatively analyze the interaction between adjacent Gd³⁺ with a large spin value of *S* = 7/2.

$$\chi_{\text{chain}} = \frac{Ng^2\beta^2}{3kT} \frac{1+u}{1-u} S(S+1) \quad (1)$$

$$u = \coth(J_c S(S+1)/kT) - kT/J_c S(S+1)$$

In eqn (1), *N* is Avogadro's number, β is the Bohr magneton, *k* is the Boltzmann constant, and *J_c* is the exchange coupling parameter between adjacent spins. The best fitting of the susceptibility data for 3 gives *g* = 1.992, *J_c* = -0.02 cm⁻¹, and the agreement factor $R = \sum[(\chi_M T)_{\text{obsd}} - (\chi_M T)_{\text{calcd}}]^2 / \sum[(\chi_M T)_{\text{obsd}}]^2 = 2.29 \times 10^{-5}$. The negative and small *J_c* value indicates that very weak antiferromagnetic coupling exists between adjacent Gd³⁺, consistent with the previous reports.^{21,22} The negative value of $\theta = -0.69$ K (Fig. S4†) obtained from the Curie–Weiss fitting further proved the existence of antiferromagnetic interaction in compound 3.

For 4–6, the $\chi_M T$ values of 11.61, 14.05 and 13.83 cm³ K mol⁻¹ at room temperature, are consistent with the corresponding expected values of uncoupled Tb³⁺ (*S* = 3, *L* = 3, ⁷F₆, *g* = 3/2, $\chi_M T$ = 11.82 cm³ K mol⁻¹), Dy³⁺ (*S* = 5/2, *L* = 5, ⁶H_{15/2}, *g* = 4/3, $\chi_M T$ = 14.17 cm³ K mol⁻¹) and Ho³⁺ (*S* = 5/4, $\chi_M T$ = 14.07 cm³ K mol⁻¹), respectively. Upon cooling, the $\chi_M T$ values of 4 and 5 keep unchanged, and for 6, it gradually declines. Then the $\chi_M T$ values undergo a more sudden reduction at temperatures below 50 K, reaching values of 6.61, 11.34 and 10.82 cm³ K mol⁻¹ for 4–6, respectively. The

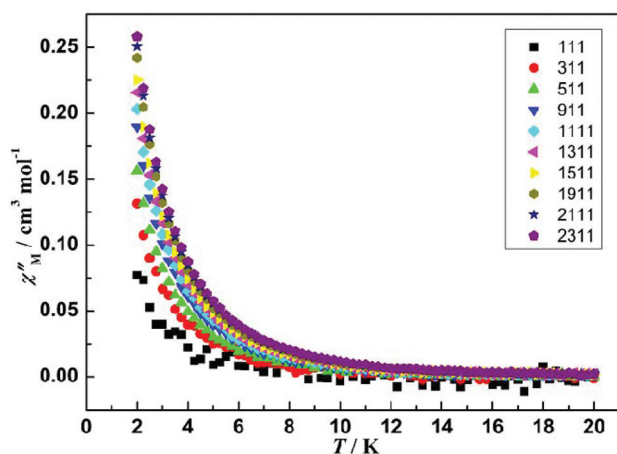


Fig. 7 Temperature dependence of the out-of-phase (χ'') ac susceptibilities for **5** at the indicated frequencies.

unchanged $\chi_M T$ values of **4** and **5** between 300 K–100 K indicate ferromagnetic interactions must operate in them, which compensate the dropping of $\chi_M T$ values caused by the depopulation of the Stark sublevels of Ln^{3+} . Similarly, the downtrend of $\chi_M T$ in **6** could not prove the presence of antiferromagnetic interaction.^{9a}

In consideration of the single-molecule magnet (SMM) behavior in previous Dy-compounds, the frequency and temperature dependencies of the alternating current (ac) susceptibilities have been investigated under zero direct current (dc) field for compound **5** (Fig. S5[†] and Fig. 7). These data show a frequency dependent out-of-phase signals below about 10 K, indicating that **5** exhibits a slow magnetic relaxation behavior. However, there are no peaks in the out-of-phase susceptibility data in the temperature range technically available, which is frequently observed in the Dy-based compounds.²³ Hence, the energy barrier of the system cannot be procured by Arrhenius formula fitting. Supposed that there is only one relaxation process in **5**, the Debye model and equation²⁴: $\ln(\chi''/\chi') = \ln(\omega\tau_0) + E_a/k_B T$ could be applied, giving the rough energy barrier $E_a/k_B \approx 1.82$ K and the pre-exponential factor $\tau_0 \approx 2.11 \times 10^{-6}$ s (Fig. S6[†]), which is in the normal range of 10^{-6} – 10^{-11} s for SMMs.²⁵

Conclusions

In summary, seven lanthanide coordination polymers have been synthesized *via* hydrothermal method, and a series of characterizations and properties have been measured. Compounds **2**, **4** and **5** emit the characteristic emissions of Eu^{3+} , Tb^{3+} and Dy^{3+} , respectively, and their corresponding luminescence lifetimes are 0.53, 0.99 and 0.014 ms. Magnetic investigations reveal that compound **3** displays antiferromagnetic interaction, **4** and **5** exhibit ferromagnetic coupling, and compound **5** exhibits a slow magnetic relaxation behavior. The calculation by the Debye model gives the energy barrier $E_a/k_B \approx 1.82$ K and the pre-exponential factor $\tau_0 \approx 2.11 \times 10^{-6}$ s for **5**.

Acknowledgements

This work was supported by the 973 Program (2012CB821702 and 2011CB935902), and NSFC (91122004 and 21271137).

Notes and references

- (a) F. A. Paz, J. Klinowski, S. M. Vilela, J. P. Tome, J. A. Cavaleiro and J. Rocha, *Chem. Soc. Rev.*, 2012, **41**, 1088; (b) G. Férey, *Chem. Soc. Rev.*, 2008, **37**, 191; (c) M. Kawano, T. Kawamichi, T. Haneda, T. Kojima and M. Fujita, *J. Am. Chem. Soc.*, 2007, **129**, 15418; (d) C. D. Wu and W. B. Lin, *Angew. Chem., Int. Ed.*, 2005, **44**, 1958; (e) B. Moulton and M. J. Zaworotko, *Chem. Rev.*, 2001, **101**, 1629.
- (a) P. Cui, Y. G. Ma, H. H. Li, B. Zhao, J. R. Li, P. Cheng, P. B. Balbuena and H. C. Zhou, *J. Am. Chem. Soc.*, 2012, **134**, 18892; (b) P. Cui, L. J. Ren, Z. Chen, H. C. Hu, B. Zhao, W. Shi and P. Cheng, *Inorg. Chem.*, 2012, **51**, 2303; (c) E. Haldoupis, S. Nair and D. S. Sholl, *J. Am. Chem. Soc.*, 2010, **132**, 7528; (d) M. Eddaoudi, J. Kim, N. Rosi, D. Vodak, J. Wachter, M. O'Keeffe and O. M. Yaghi, *Science*, 2002, **295**, 469; (e) O. M. Yaghi, H. Li, M. Eddaoudi and M. O'Keeffe, *Nature*, 1999, **402**, 276.
- (a) M. Gustafsson, A. Bartoszewicz, B. N. Martín-Matute, J. Sun, J. Grins, T. Zhao, Z. Y. Li, G. S. Zhu and X. D. Zou, *Chem. Mater.*, 2010, **22**, 3316; (b) M. J. Vitorino, T. Devic, M. Tromp, G. Férey and M. Visseaux, *Macromol. Chem. Phys.*, 2009, **210**, 1923; (c) F. Gándara, B. Gomez-Lor, E. Gutiérrez-Puebla, M. Iglesias, M. A. Monge, D. M. Proserpio and N. Snejko, *Chem. Mater.*, 2008, **20**, 72; (d) M. Müller, S. Hermes, K. Kähler, M. W. E. Vanden Berg, M. Muhler and R. A. Fischer, *Chem. Mater.*, 2008, **20**, 4576.
- (a) G. Lu and J. T. Hupp, *J. Am. Chem. Soc.*, 2010, **132**, 7832; (b) B. L. Chen, L. B. Wang, Y. Q. Xiao, F. R. Fronczek, M. Xue, Y. J. Cui and G. D. Qian, *Angew. Chem., Int. Ed.*, 2009, **48**, 500; (c) B. Zhao, X. Y. Chen, Z. Chen, W. Shi, P. Cheng, S. P. Yan and D. Z. Liao, *Chem. Commun.*, 2009, 3113; (d) B. L. Chen, L. B. Wang, F. Zapata, G. D. Qian and E. B. Lobkovsky, *J. Am. Chem. Soc.*, 2008, **130**, 6718; (e) B. Zhao, X. Y. Chen, P. Cheng, D. Z. Liao, S. P. Yan and Z. H. Jiang, *J. Am. Chem. Soc.*, 2004, **126**, 15394.
- (a) K. C. Stylianou, R. Heck, S. Y. Chong, J. Bacsa, J. T. Jones, Y. Z. Khimiyak, D. Bradshaw and M. J. Rosseinsky, *J. Am. Chem. Soc.*, 2010, **132**, 4119; (b) D. W. Fu, W. Zhang and R. G. Xiong, *Dalton Trans.*, 2008, 3946; (c) Y. Liu, G. Li, X. Li and Y. Cui, *Angew. Chem., Int. Ed.*, 2007, **46**, 6301; (d) O. R. Evans and W. Lin, *Acc. Chem. Res.*, 2002, **35**, 511.
- G. Férey, F. Millange, M. Morcrette, C. Serre, M. L. Doublet, J. M. Grenéche and J. M. Tarascon, *Angew. Chem., Int. Ed.*, 2007, **46**, 3259.
- (a) P. F. Shi, G. Xiong, B. Zhao, Z. Y. Zhang and P. Cheng, *Chem. Commun.*, 2013, **49**, 2338; (b) Y. Liu, Z. Chen, J. Ren, X. Q. Zhao, P. Cheng and B. Zhao, *Inorg. Chem.*, 2012, **51**,

- 7433; (c) P. F. Shi, Y. Z. Zheng, X. Q. Zhao, G. Xiong, B. Zhao, F. F. Wan and P. Cheng, *Chem.–Eur. J.*, 2012, **18**, 15086; (d) X. Q. Zhao, B. Zhao, W. Shi and P. Cheng, *Inorg. Chem.*, 2009, **48**, 11048; (e) B. Zhao, H. L. Gao, X. Y. Chen, P. Cheng, W. Shi, D. Z. Liao, S. P. Yan and Z. H. Jiang, *Chem.–Eur. J.*, 2006, **12**, 149.
- 8 (a) J. J. Morris, B. C. Noll and K. W. Henderson, *Chem. Commun.*, 2007, 5191; (b) Y. L. Hou, G. Xiong, P. F. Shi, R. R. Cheng, J. Z. Cui and B. Zhao, *Chem. Commun.*, 2013, **49**, 6066; (c) Z. Chen, B. Zhao, P. Cheng, X. Q. Zhao, W. Shi and Y. Song, *Inorg. Chem.*, 2009, **48**, 3493; (d) J. Rocha, L. D. Carlos, F. A. Paz and D. Ananias, *Chem. Soc. Rev.*, 2011, **40**, 926; (e) J. Xia, B. Zhao, H. S. Wang, W. Shi, Y. Ma, H. B. Song, P. Cheng, D. Z. Liao and S. P. Yan, *Inorg. Chem.*, 2007, **46**, 3450; (f) X. Yang and R. A. Jones, *J. Am. Chem. Soc.*, 2005, **127**, 7686; (g) Y. P. Ren, L. S. Long, B. W. Mao, Y. Z. Yuan, R. B. Huang and L. S. Zheng, *Angew. Chem., Int. Ed.*, 2003, **42**, 532.
- 9 (a) Y. L. Hou, G. Xiong, B. Shen, B. Zhao, Z. Chen and J. Z. Cui, *Dalton Trans.*, 2013, **42**, 3587; (b) J. Xu, W. P. Su and M. C. Hong, *Cryst. Growth Des.*, 2011, **11**, 337; (c) D. Aguilà, L. A. Barrios, F. Luis, A. Repollés, O. Roubeau, S. J. Teat and G. Aromí, *Inorg. Chem.*, 2010, **49**, 6784.
- 10 (a) P. F. Shi, B. Zhao, G. Xiong, Y. L. Hou and P. Cheng, *Chem. Commun.*, 2012, **48**, 8231; (b) P. J. Deren, R. Mahiou, W. Strek, A. Bednarkiewicz and G. Bertrand, *Opt. Mater.*, 2002, **19**, 145.
- 11 (a) M. V. Lucky, S. Sivakumar, M. L. P. Reddy, A. K. Paul and S. Natarajan, *Cryst. Growth Des.*, 2011, **11**, 857; (b) Y. Li, F. K. Zheng, X. Liu, W. Q. Zou, G. C. Guo, C. Z. Lu and J. S. Huang, *Inorg. Chem.*, 2006, **45**, 6308; (c) X. He, X. P. Lu, Z. F. Ju, C. J. Li, Q. K. Zhang and M. X. Li, *CrystEngComm*, 2013, **15**, 2731; (d) J. Yang, S. Y. Song, J. F. Ma, Y. Y. Liu and Z. T. Yu, *Cryst. Growth Des.*, 2011, **11**, 5469; (e) P. Lama, A. Aijaz, S. Neogi, L. J. Barbour and P. K. Bharadwaj, *Cryst. Growth Des.*, 2010, **10**, 3410; (f) R. Cao, D. F. Sun, Y. C. Liang, M. C. Hong, K. Tatsumi and Q. Shi, *Inorg. Chem.*, 2002, **41**, 2087.
- 12 G. Sheldrick, *Acta Crystallogr., Sect. A: Fundam. Crystallogr.*, 2008, **64**, 112.
- 13 (a) B. M. Ji, D. S. Deng, X. He, B. Liu, S. B. Miao, N. Ma, W. Z. Wang, L. G. Ji, P. Liu and X. F. Li, *Inorg. Chem.*, 2012, **51**, 2170; (b) W. Huang, D. Y. Wu, P. Zhou, W. B. Yan, D. Guo, C. Y. Duan and Q. J. Meng, *Cryst. Growth Des.*, 2009, **9**, 1361; (c) H. S. Wang, B. Zhao, B. Zhai, W. Shi, P. Cheng, D. Z. Liao and S. P. Yan, *Cryst. Growth Des.*, 2007, **7**, 1851; (d) A. F. Kirby, D. Foster and F. S. Richardson, *Chem. Phys. Lett.*, 1983, **95**, 507.
- 14 C. X. Du, Z. Q. Wang, Q. Xin, Y. J. Wu and W. L. Li, *Acta Chim. Sin.*, 2004, **62**, 2265.
- 15 (a) R. Łyszczek and A. Lipke, *Microporous Mesoporous Mater.*, 2013, **168**, 81; (b) T. F. Liu, W. Zhang, W. H. Sun and R. Cao, *Inorg. Chem.*, 2011, **50**, 5242; (c) Z. H. Zhang, Y. Song, T. Okamura, Y. Hasegawa, W. Y. Sun and N. Ueyama, *Inorg. Chem.*, 2006, **45**, 2896; (d) Y. B. Wang, W. J. Zhuang, L. P. Jin and S. Z. Lu, *J. Mol. Struct.*, 2005, **737**, 165.
- 16 (a) Q. Y. Liu, W. F. Wang, Y. L. Wang, Z. M. Shan, M. S. Wang and J. K. Tang, *Inorg. Chem.*, 2012, **51**, 2381; (b) M. X. Wang, L. S. Long, R. B. Huang and L. S. Zheng, *Chem. Commun.*, 2011, **47**, 9834; (c) S. Sivakumar, M. L. Reddy, A. H. Cowley and R. R. Butorac, *Inorg. Chem.*, 2011, **50**, 4882; (d) V. I. Tsaryuk, K. P. Zhuravlev, A. V. Vologzhanina, V. A. Kudryashova and V. F. Zolin, *J. Photochem. Photobiol., A*, 2010, **211**, 7; (e) A. de Bettencourt-Dias, P. S. Barber, S. Viswanathan, D. T. de Lill, A. Rollett, G. Ling and S. Altun, *Inorg. Chem.*, 2010, **49**, 8848; (f) P. C. Soares-Santos, L. Cunha-Silva, F. A. Paz, R. A. Ferreira, J. Rocha, L. D. Carlos and H. I. Nogueira, *Inorg. Chem.*, 2010, **49**, 3428; (g) S. Viswanathan and A. Bettencourt-Dias, *Inorg. Chem.*, 2006, **45**, 10138.
- 17 W. X. Li, Y. S. Zheng, X. J. Sun, W. J. Chai, T. Ren and X. Y. Shi, *J. Lumin.*, 2010, **130**, 1455.
- 18 (a) Y. Luo, G. Calvez, S. Freslon, K. Bernot, C. Daugebonne and O. Guillou, *Eur. J. Inorg. Chem.*, 2011, 3705; (b) C. Daugebonne, N. Kerbellec, O. Guillou, J. C. Bunzli, F. Gummy, L. Catala, T. Mallah, N. Audebrand, Y. Gerault, K. Bernot and G. Calvez, *Inorg. Chem.*, 2008, **47**, 3700.
- 19 (a) P. Pekarkova, Z. Spichal, P. Taborsky and M. Necas, *Luminescence*, 2011, **26**, 650; (b) M. H. V. Werts, R. T. F. Jukes and J. W. Verhoeven, *Phys. Chem. Chem. Phys.*, 2002, **4**, 1542.
- 20 M. E. Fisher, *Am. J. Phys.*, 1964, **32**, 343.
- 21 N. Xu, W. Shi, D. Z. Liao, S. P. Yan and P. Cheng, *Inorg. Chem.*, 2008, **47**, 8748.
- 22 (a) F. S. Guo, J. D. Leng, J. L. Liu, Z. S. Meng and M. L. Tong, *Inorg. Chem.*, 2012, **51**, 405; (b) X. Feng, J. Wang, B. Liu, L. Wang, J. S. Zhao and S. Ng, *Cryst. Growth Des.*, 2012, **12**, 927; (c) H. C. Liu, I. H. Chen, A. Huang, S. C. Huang and K. F. Hsu, *Dalton Trans.*, 2009, 3447.
- 23 (a) Y. Wang, X. L. Li, T. W. Wang, Y. Song and X. Z. You, *Inorg. Chem.*, 2010, **49**, 969; (b) H. S. Ke, G. F. Xu, L. Zhao, J. K. Tang, X. Y. Zhang and H. J. Zhang, *Chem.–Eur. J.*, 2009, **15**, 10335; (c) Y. Z. Zheng, Y. Lan, C. E. Anson and A. K. Powell, *Inorg. Chem.*, 2008, **47**, 10813; (d) M. T. Gamer, Y. Lan, P. W. Roesky, A. K. Powell and R. Clerac, *Inorg. Chem.*, 2008, **47**, 6581.
- 24 (a) S. Y. Lin, G. F. Xu, L. Zhao, Y. N. Guo, Y. Guo and J. K. Tang, *Dalton Trans.*, 2011, **40**, 8213; (b) J. Bartolomé, G. Filoti, V. Kuncser, G. Schinteie, V. Mereacre, C. E. Anson, A. K. Powell, D. Prodius and C. Turta, *Phys. Rev. B: Condens. Matter*, 2009, **80**, 014430.
- 25 Y. L. Miao, J. L. Liu, J. Y. Li, J. D. Leng, Y. C. Ou and M. L. Tong, *Dalton Trans.*, 2011, **40**, 10229.